ISSN 1819-7140, Russian Journal of Pacific Geology, 2022, Vol. 16, No. 4, pp. 300–316. © Pleiades Publishing, Ltd., 2022.
Russian Text © The Author(s), 2022, published in Tikhookeanskaya Geologiya, 2022, Vol. 41, No. 4, pp. 23–40.

Taking a Fresh Look at the Stratigraphy of the Selemdzha and Tokur Terranes of the Mongol–Okhotsk Belt: The Results of U–Pb, Lu–Hf, and Sm–Nd Isotope Studies

V. A. Zaika[a], *, A. Yu. Kadashnikova[a], and A. A. Sorokin[a]

[a] *Institute of Geology and Nature Management, Far Eastern Branch, Russian Academy of Sciences, Blagoveshchensk, 675000 Russia*

**e-mail: zaika_v_a_88@mail.ru*

Received January 17, 2021; revised January 21, 2022; accepted March 16, 2022

Abstract—The results from U–Pb, Lu–Hf, and Sm–Nd isotope studies of metasedimentary rocks from the Selemdzha and Tokur terranes of the Mongol–Okhotsk belt contradict the existing concepts on the stratigraphy of the region and indicate the need to revise the traditional principles of mapping within the belt. Two types of deposits that sharply differ in their Sm–Nd whole-rock characteristics and Lu–Hf isotope compositions of detrital zircons have been established within the terranes. Deposits of different types are involved in the formation of the two opposite accretionary systems: in front of the Siberian Craton margin (type I) and the Amur superterrane (type II). The type I deposits are divided into groups with different lower age limits: 553–498 Ma, Late Ediacaran–Cambrian; ~373 Ma, Upper Devonian; 333–327 Ma, Upper Mississippian; and ~304 Ma, Pennsylvanian. The deposits of the tectonic-stratigraphic units show a general trend of decreasing age from north southward. The same trend is observed from the upper to lower sheets. Such a structure is typical of accretionary wedge-shaped terranes with a rear part in the north and a frontal part in the south. The tectonic-stratigraphic units formed by type I deposits and previously ascribed to the Selemdzha and Tokur terranes likely belong to the Galam accretionary wedge terrane.

Keywords: U–Pb, Lu–Hf, Sm–Nd, stratigraphy, Tokur terrane, Selemdzha terrane, Mongol-Okhotsk fold belt

DOI: 10.1134/S181971402204008X

INTRODUCTION

The Mongol–Okhotsk fold belt is one of the major structural units of East Asia. It is extended as a narrow (up to 300 km) band for 3000 km from Uda Bay of the Okhotsk Sea to Central Mongolia (Fig. 1). In the modern structural plan, the belt is a composite collage extended along the strike of tectonic blocks, which are considered as lithotectonic zones [12, 16, 19] or terranes [5, 6, 17, 36, 37, and others]. At present, the Mongol–Okhotsk fold belt is thought to be a relict of the eponymous paleoocean, which closed during collision of the North Asian craton and Amur superterrane [6, 13, 17, and others].

The evolution of the Mongol–Okhotsk belt has been studied for over 50 years, but many cardinal problems remained unsolved [5, 17, 18, 33, and others]. Thus, the most controversial problems are the age and relationships of geological complexes that compose this belt, as well as timing and style of accretionary and collision processes.

Complex U–Pb, Lu–Hf, Sm–Nd isotope studies of sedimentary rocks of the belt are an efficient tool for solving these problems. In particular, it was recently established that sedimentary complexes of the Mongol–Okhotsk belt do not contain detrital zircons younger than 171 Ma [8, 9, 40, 47], but zircons of such ages are present in the rocks of the Jurassic orogenic depressions on both sides of the Mongol–Okhotsk belt [10, 20]. This fact, as well as results of recent paleomagnetic studies [46], indicate that sedimentation in the Mongol–Okhotsk basin was terminated at the Early–Middle Jurassic boundary owing to its closure and formation of orogenic buildup on its site. A similar conclusion was obtained by Sm–Nd study of the rocks of the Irkutsk sedimentary basin [26].

In addition, the study of detrital zircons from Paleozoic sedimentary complexes of the Adaatsag, Doschgol, Hangai-Hentei, and Ereendava terranes from the western part [25, 29, 31, 39], as well as the Yankan, Tukuringra, Un'ya-Bom, Dzhagdy, Lan, and Selemdzha terranes from the eastern part [9, 40, 47] of the Mongol–Okhotsk belt indicates the existence of opposite subduction zones in the Paleozoic and Early Mesozoic.

At the same time, the results of U–Pb, Lu–Hf, and Sm–Nd isotope studies of sedimentary deposits of the

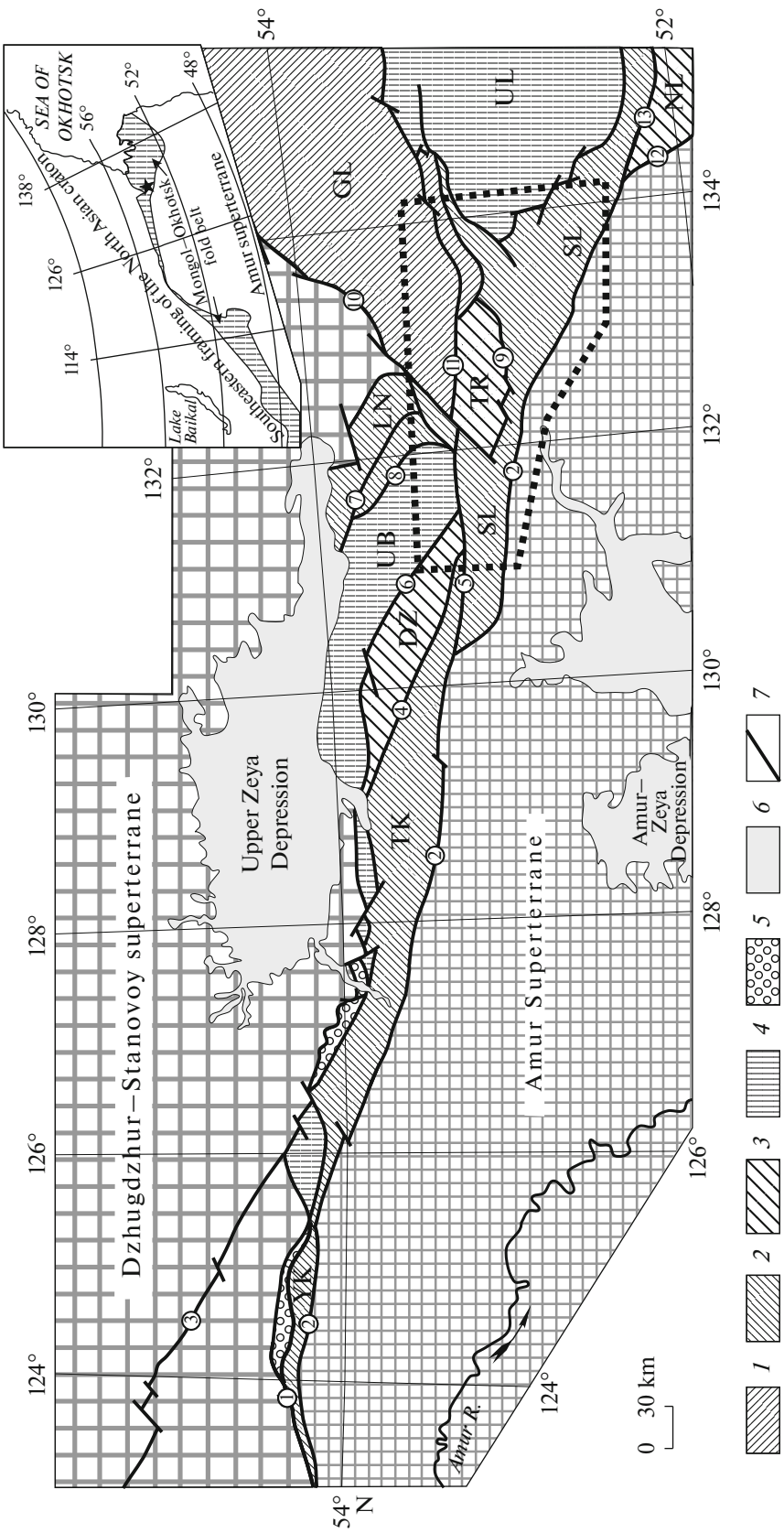

Fig. 1. The terrane scheme of the eastern Mongol–Okhotsk fold belt after [21]. (*1*) terranes made up of conditionally Lower and Middle Paleozoic metasedimentary and metavolcanic complexes; (*2*) terranes made up of conditionally Middle and Upper Paleozoic metasedimentary and metavolcanic complexes; (*3*) terranes made up of conditionally Upper Paleozoic metasedimentary and metavolcanic complexes; (*4*) terranes made up of conditionally Lower Mesozoic turbidite compelxes; (*5*) Upper Jurassic–Lower Cretaceous conglomerates, gravelstones, sandstones; (*6*) Cenozoic loose deposits; (*7*) faults. Terranes are shown by the letters: (GL) Galam, (DZ) Dzhagdy, (NL) Nilan, (LN) Lan, (SL) Selemdzha, (TK) Tukuringra, (TR) Tokur; (UL) Ul'ban, (UB) Un'ya-Bom, (YK) Yankan. Circled numerals show faults after [12, 19]: (1) North Tukuringra, (2) South Tukuringra, (3) Dzheltulak, (4) Tuksi, (5) Nora, (6) Champuli, (7) Lan, (8) Ogdzhenon, (9) Tugur, (10) Uligdan, (11) Mariinsk, (12) Upper Niman, (13) Nilan. Polygons in the scheme and asterisk in inset show the studied area.

Mongol–Okhotsk belt can be used for the correlation of stratigraphic units (formations and sequences) that participate in the belt structure. Moreover, given the few and poor finds of fossil flora and fauna in these rocks, as well as intense deformation of the rocks in combination with poor exposure, isotope data become not only important, but also essential for stratigraphic studies. In particular, as we showed recently [47], the rocks of the Selemdzha and Tokur terranes in the eastern Mongol–Okhotsk belt were derived from fundamentally different sources of detrital material. This fact was used to reconstruct the fragments of accretionary complexes and to establish the dip direction of subduction zones. However, many aspects that are important for the stratigraphy of these terranes are not considered in the indicated publications.

In this paper, we attempted to demonstrate the significance and role of U–Pb, Lu–Hf, and Sm–Nd isotope studies for the critical analysis of the existing concepts on the stratigraphy of the Selemdzha and Tokur terranes, as well as for elaboration of constraints on age correlation of these deposits. Thus, factual material used in our previous paper [47] was supplemented by a great body of new isotope data.

THE GEOLOGICAL BACKGROUND

Numerous geodynamic models of the formation of the Mongol–Okhotsk belt have been developed based on different tectonic concepts. Correspondingly, numerous structural schemes have been published [5, 6, 16, 17, 36, 37, and others]. For the eastern Mongol–Okhotsk belt, we used a scheme (Fig 1) published in [21] that is close to versions proposed in [5, 17, 37] but differs in its greater detail.

Prior turning to the description of stratigraphy of the Mongol–Okhotsk belt, it is necessary to note the following. From the 1960s to the present, practically the same stratigraphic units are distinguished in the Selemdzha and Tokur terranes (structural zones). In particular, the following succession is proposed for the Selemdzha terrane (from bottom upward): Afanas'ev Formation → Talyma Formation → Zlatoust Formation → Sagur Formation; Tokur terrane: Tokur Formation → Ekimchan Formation → Bokontia Formation [1–4, 7, 12, 14, 15, 19, 22].

A single find of a spore–pollen assemblage typical of the Carboniferous Visean–Moscovian stages was recently reported for siltstones of the Zlatoust Formation (see above) [2, 12]. However, this cannot solve all the existing stratigraphic problems of the region. In addition, geological mapping in this area is complicated by intense deformations and the absence of clear criteria for distinguishing formations/sequences. For this reason, the next generation of geological maps significantly differed from the previous map not only in the age of stratigraphic units, but also in their contours.

The Selemdzha terrane (Figs. 1, 2) from the south, along the South Tukuringra fault is in contact with the northern margin of the Bureya massif, which according to the existing concepts [13, 17, 18, 33], is ascribed to the Amur superterrane. In the north, the Selemdzha terrane borders the Tukuringra, Dzhagdy, Un'ya-Bom, and Tokur terranes through a composite fault system; in the east, it joins the Ul'ban and Kerbi terranes.

The Selemdzha terrane comprises volcanogenic and sedimentary rocks that are variably metamorphosed under greenschist-facies conditions. At present, the following succession of stratified rocks is distinguished [1–3, 12]. The base is composed of the Lower Carboniferous (?) [12] or Lower Paleozoic (?) [1] *Afanas'ev Formation*, which is over 1200-m thick. It is made up of muscovite–quartz–albite, biotite–muscovite–quartz–albite, and albite—-chlorite–epidote–amphibole schists. This formation is more metamorphosed than others. It is conformably (?) overlain by the conditionally Lower Carboniferous (?) *Talyma Formation*, which is up to 1600-m thick and consists of metasandstones, metasiltstones, clayey shales, green schists, quartzites, and marbled limestones. The overlying 2100-m thick Upper Carboniferous *Zlatoust Formation* consists of clayey shales, metasandstones, and metasiltstones, green schists, metabasalts, microquartzites, and marbled limestones. *The Zlatoust Formation* was assigned to the Late Carboniferous based on the discovery of the Visean–Moscovian spore–pollen assemblage in siltstones [1, 12]. The Upper Carboniferous (?) *Sagur Formation*, which is over 1200-m thick lies conformably on the Zlatoust Formation and consists of phylltized shales, metasandstones, quartz–sericite, and epidote–actinolite–albite schists.

Intrusions of the Late Carboniferous (?) Zlatoust gabbro–plagiogranite complex are widespread within the Selemdzha terrane. This complex consists mainly of cataclased gabbros, plagiogranites, and tonalites [1–3, 12], which form bodies from a few meters to 1.5 km and up to 10 km long. The rocks of the Zlatoust complex intrude deposits of the Talyma and Zlatoust formations, and together with them are deformed and metamorphosed under greenschist-facies conditions [1–3, 12].

The available U–Pb geochronological data on zircons from granitoids of the Zlatoust complex are 271 ± 5 [1–3] and 269 ± 2 Ma [21]. In addition, recent U–Pb zircon dating yielded 393 ± 7, 257 ± 4, 252 ± 3, and 250 ± 4 Ma [41], which clearly indicates that this complex erroneously includes rocks of different ages.

The Tokur terrane (Figs. 1, 2) is separated from the Galam terrane by the Mariinsk Fault in the north, and is in contact with the Selemdzha terrane along the Tugur Fault in the south.

The Tokur terrane includes [2, 7, 12] the following stratigraphic units (from bottom upward). The Upper Permian (?) *Tokur Formation* 1800 m thick consists of

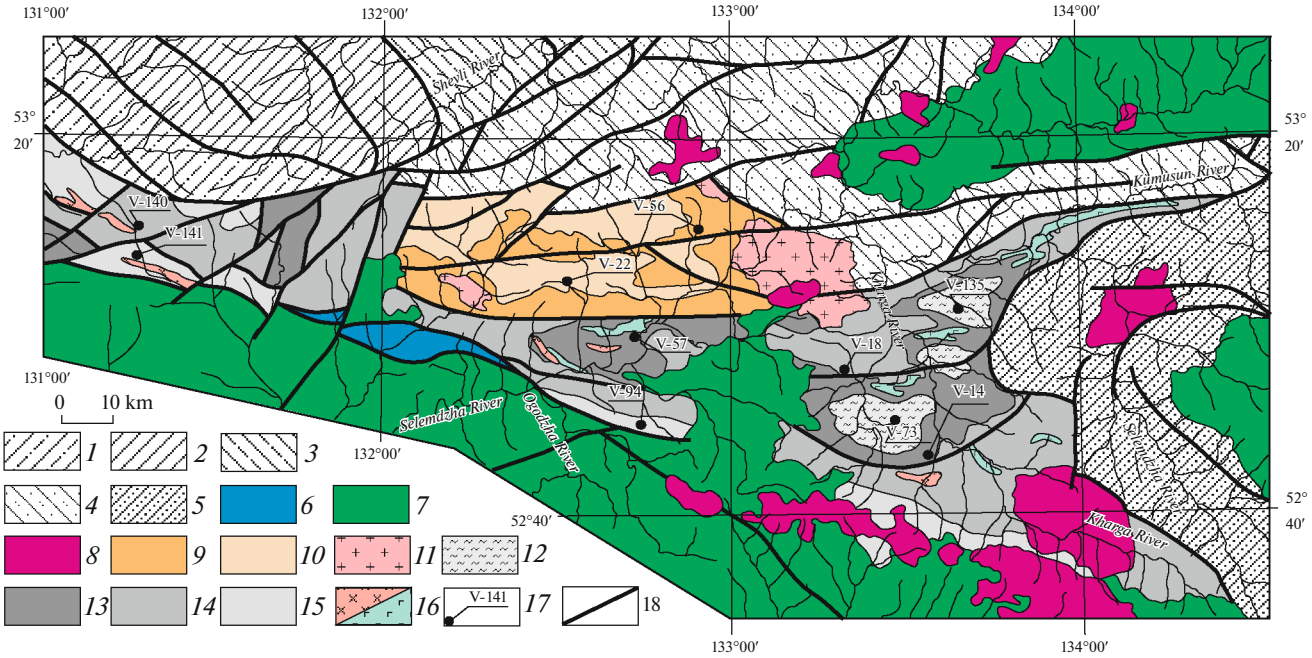

Fig. 2. The geological scheme of the Tokur and Selemdzha terranes of the Mongol–Okhotsk belt (simplified after [12, 19]). (*1–5*) structures bordering the Tokur and Selemdzha terranes: (1) Paleozoic (?) complexes of the Dzhagdy terrane; (*2*) Early Mesozoic complexes of the Un'ya–Bom terrane; (*3*) Paleozoic and Early Mesozoic complexes of the Lan terrane; (*4*) Paleozoic complexes of the Galam terrane; (*5*) Early Mesozoic complexes of the Ul'ban terrane; (*6*) Jurassic terrigenous deposits; (*7–8*) superimposed and cross-cutting Late Mesozoic magmatic complexes: (*7*) Early Cretaceous volcanic and subvolcanic complexes; (*8*) Early and Late Cretaceous intrusive complexes; (*9–11*) Paleozoic complexes of the Tokur terrane: (*9*) Upper Permian (?) Tokur Formation; (*10*) Upper Permian (?) undivided Ekimchan and Bokontia formation; (*11*) Late Paleozoic Ingagli granitoid complex; (*12–16*) Paleozoic rocks of the Selemdzha terrane: (*12*) Lower Carboniferous (?) Afanas'ev Formation; (*13*) Lower Carboniferous (?) Talyma Formation; (*14*) Upper Carboniferous Zlatoust Formation; (*15*) Upper Carboniferous (?) Sagur Formation; (*16*) Late Paleozoic Zlatoust gabbroplagiogranite complex; (*17*) sampling localities for U–Pb geochronological and Lu-Hf isotope studies; (*18*) main faults.

frequently alternating metasandstones, clay shales, and metasiltstones, with less common green schists and sedimentation breccias. The Upper Permian (?) *Ekimchan Formation* 800 m thick conformably overlies the Tokur Formation. It is made up of clay shales, metasiltstones, and units of their rhythmic alternation [2, 12]. The overlying 2150-m thick Upper Permian (?) *Bokontia Formation* consists of metasandstones, metasiltstones, clay shales, units of their rhythmic alternation, sedimentation breccias, and conglomerates. The Ekimchan and Bokontia formations have similar compound and are united in the maps of the last generation [12].

The sedimentary rocks that compose the Tokur terrane are highly deformed in folds and metamorphosed under greenschist-facies conditions. The Tokur formation is intruded by granodiorites, granites, leucogranites of the Ingagli complex, which define the U–Pb zircon ages of 254 ± 4, 251 ± 3 Ma [1–3, 12], 253 ± 2, and 253 ± 3 Ma [41].

ANALYTICAL METHODS AND SAMPLING

Sm–Nd isotope studies were performed at the Institute of Precambrian Geology and Geochronology, Russian Academy of Sciences, in St. Petersburg. A 100 mg-aliquot of powdered sample was mixed with a ^{149}Sm-^{150}Nd spike and decomposed in a Teflon vessel, in an HCl + HF + HNO_3 mixture at 110°C. The completeness of dissolution was controlled under a binocular microscope. REE were separated on BioRad AG1-X8 200–400 mesh resin using the conventional cation exchange technique. Sm and Nd were separated by extraction chromatography with an LN-Spec 100–150 mesh Eichrom resin. The isotope compositions of Sm and Nd were determined on a TRITON TI multicollector mass-spectrometer in static mode. The measured $^{143}Nd/^{144}Nd$ ratios were normalized to $^{146}Nd/^{144}Nd = 0.7219$ and adjusted relative to $^{143}Nd/^{144}Nd = 0.512115$ in the JNdi-1 Nd standard [43]. The weighted average $^{143}Nd/^{144}Nd$ ratio of ten JNdi-1 standard runs during the measurements was 0.512108 ± 7 ($n = 10$). The precision of the Sm and Nd contents is ± 0.5%, those of $^{147}Sm/^{144}Nd$ and $^{143}Nd/^{144}Nd$ are ±0.5% and ±0.005% (2σ). The total laboratory blanks were no more than 0.2 ng Sm and 0.5 ng Nd. The $\varepsilon_{Nd(t)}$ values and model ages $t_{Nd(DM)}$ were calculated using the present-day values for a chondritic uniform reservoir (CHUR) after [30]

Table 1. The affiliation of the studied samples to stratigraphic units in maps of different generations.

Sample no.	Rock	Generation of geological maps				Note
		Scale 1 : 200000	Scale 1 : 200000	Scale 1 : 500000	Scale 1 : 1000000	
		[7, 14, 22]	[1–3]	[4, 15]	[12, 19]	
V-22	Metasiltstones	Ekimchan	Ekimchan	Ekimchan	Ekimchan and Bokontia	[47]
V-56	Metasandstone	Ekimchan	Bokontia	Tokur	Tokur	[47]
V-94	Metasiltstones	Tokur	Sagur	Zlatoust	Sagur	[47]
V-141	Metasiltstones	Zlatoust	Sagur	Zlatoust	Sagur	This study
V-140	Metasiltstones	Zlatoust	Zlatoust	Zlatoust	Zlatoust	This study
V-14	Metasiltstones	Talyma	Talyma	Talyma	Talyma	[47]
V-18	Metasiltstones	Talyma	Zlatoust	Zlatoust	Zlatoust	[47]
V-57	Metasiltstones	Sagur	Sagur	Zlatoust	Talyma	[47]
V-73	Two-mica schist	Afanas'ev	Afanas'ev	Afanas'ev	Afanas'ev	[47]
V-135	Two-mica schist	Afanas'ev	Afanas'ev	Afanas'ev	Afanas'ev	This study

($^{143}Nd/^{144}Nd = 0.512638$, $^{147}Sm/^{144}Nd = 0.1967$) and DM after [28] ($^{143}Nd/^{144}Nd = 0.513151$, $^{147}Sm/^{144}Nd = 0.21365$). To account for the possible Sm and Nd fractionation in intracrustal processes, the two-stage Nd model ages $t_{Nd(C)}$ [32] were calculated using a mean crustal ratio of $^{147}Sm/^{144}Nd = 0.12$ [44].

Detrital zircons were separated at the Institute of Geology and Nature Management of the Far Eastern Branch of the Russian Academy of Sciences (Blagoveshchensk) using a heavy liquid technique. The U–Pb geochronological studies of separate zircons were carried out by the laser-ablation–inductively coupled plasma mass spectrometry (LA–ICP–MS) at the Arizona LaserChron Center, Department of Geosciences, University of Arizona, United States, using a Thermo Element 2 mass spectrometer equipped with a Photon Machines Analyte G2 laser ablation system. The crater was 20 μm across and 15 μm deep. Calibration was carried out using FS standard (Duluth complex, 1099.3 ± 0.3 Ma [38]). The Sri Lanka (SL) and Braintree complex (R33) standards were used as secondary standards for quality control [23]. The $^{206}Pb/^{238}U$ and $^{207}Pb/^{206}Pb$ ages for SL zircon during measurements were 57 ± 5 and 558 ± 7 Ma (2σ), respectively, which is consistent with the values published in [27] obtained using the ID-TIMS method. The average $^{206}Pb/^{238}U$ and $^{207}Pb/^{206}Pb$ ages for the R33 standard were 417 ± 7 and 415 ± 8 Ma, which correspond to the recommended values [23, 35]. The systematic errors were 0.9% for $^{206}Pb/^{238}U$ and 0.8% for $^{206}Pb/^{207}Pb$ (2σ). Correction for common Pb was introduced using ^{204}Pb corrected for ^{204}Hg according to the model values [42]. The following U decay constants were as follows: $^{238}U = 9.8485 \times 10^{-10}$, $^{235}U = 1.55125 \times 10^{-10}$, $^{238}U/^{235}U = 137.88$. A detailed description of the analytical procedures is given at site of the Arizona LaserChron Center of Arizona University (www.laserchron.org). Concordant ages were calculated in Isoplot v. 4.15 software [34] and were used to plot the relative-age probability diagrams for detrital zircons.

Lu–Hf isotope analyses of zircons were carried out at the same laboratory using a multicollector Nu High-Resolution ICP mass spectrometer connected to an Analyte G2 excimer laser. The analytical technique was reported in detail at the site of the Arizona LaserChron Center (www.laserchron.org). The $\varepsilon_{Hf(t)}$ values were calculated using chondrite $^{176}Hf/^{177}Hf$ (0.282785) and $^{176}Lu/^{177}Hf$ (0.0332) ratios according to [24], as well as U–Pb ages obtained for individual grains. Crustal Hf model ages $t_{Hf(C)}$ were calculated taking the average $^{176}Lu/^{177}Hf$ of 0.0093 in continental crust [45].

Samples were collected to characterize all distinguished stratigraphic units by isotope studies. However, this procedure was complicated by the fact that the outlines of stratones on maps of different generations significantly differ, as mentioned above. Our studies were based on the maps of last generation (Fig. 2) [12, 19]. At the same time, Table 1 demonstrates the affiliation of all studied samples, including previously analyzed samples [47] and used in section Discussion, to definite formations in maps of all generations.

In the framework of this study, we performed Sm–Nd isotope studies of weakly metamorphosed sedimentary rocks of four samples in addition to 14 previously analyzed samples [47], as well as U–Pb and Lu–Hf isotope studies of detrital zircons in three samples in addition to seven previously analyzed samples [47]. A brief description of samples used for geochronological studies in this work is given in Table 2, while their sampling localities are shown in Fig. 2.

Table 2. A brief description and sampling localities.

Sample no.	Coordinates	Formation	Lithological description
V-135	133°30′26.8″ E 53°50′04.1″ N	Afanas'ev Formation	Gray biotite–muscovite–albite schists with porphyroblastic texture; angular to subangular clastic material 2–5 mm in size: quartz (25–30%), albite (35–40%), biotite (10–15%), muscovite (3–7%)
V-140	131°13′32.5″ E 53°09′44.4″ N	Zlatoust Formation	Dark gray siltstones with psammitic fine-grained texture; angular and subrounded clastic material 0.01–0.03 mm in size: quartz (25–30%), plagioclase (25–30%), rock fragments (15–20%), sericite (5–7%)
V-141	131°14′13.1″ E 53°08′10.2″ N	Sagur Formation	Gray siltstones with psammitic fine-grained texture: angular and subrounded clastic material 0.02–0.05 mm in size: quartz (25–30%) rock fragments (15–20%), plagioclase (25–30%), sericite (3–5%)

THE RESULTS OF U–Pb GEOCHRONOLOGICAL STUDIES

The U–Pb isotope results are shown in Fig. 3 and Supplement_1.

Sample V-135: biotite–muscovite–quartz–albite schist of the Afanas'ev Formation. From this sample, we analyzed 130 zircons, 115 of which yielded concordant ages (Fig. 3a). The majority of the zircons have a Paleoproterozoic age with age peaks at ~2.02 and 1.90 Ga in the relative-age probability diagram. There are also numerous Paleozoic (peaks at 510, 492, 384, and 339 Ma), Neoproterozoic (peaks at 897 and 594 Ma), and Archean (peak at 2.55 Ga) zircons. The concordant age of the youngest population is 333 ± 3 Ma.

Sample V-140 is the metasiltstone from the Zlatoust Formation. Of 121 analyzed 121 zircons, 104 zircons yielded concordant ages (Fig. 3e). The predominant part of zircons has Neoproterozoic age with peaks at ~886, ~804, 618, and 577 Ma in the relative-age probability diagram. There are also numerous Paleoproterozoic zircons with peak values at 1.97, 1.92, 1.74, and 1.64 Ga. Paleozoic zircons occur in subordinate amount (peaks at 522 and 501 Ma). The youngest zircon population has a concordant age of 501 ± 5 Ma.

Sample V-141: metasiltstones of the Sagur Formation. Of 123 analyzed zircons, 110 zircons gave concordant ages (Fig. 3g). They are mainly characterized by the Neoproterozoic age with peaks at 883, 805, and 575 Ma in the relative-age probability diagram, with less common Paleoproterozoic zircons peaked at 1.99, 1.88, and 1.71 Ga. Paleozoic zircons occur in subordinate amount (peak at 513 Ma). The youngest zircons have a concordant age of 498 ± 4 Ma.

THE RESULTS OF LU-HF ISOTOPE STUDIES

The results of Lu–Hf isotope studies are given in Fig. 4 and in Supplementary_2. As follows from these results, Paleoproterozoic zircons in all studied samples are characterized by the negative and weakly positive values of $\varepsilon_{Hf(t)}$ from –7.5 to +4.9 and two stage model ages of $t_{Hf(C)} > 1.92$ Ga. Neoproterozoic and Cambrian zircons in these samples, in contrast, have weakly negative and positive values of $\varepsilon_{Hf(t)}$ from –5.1 to +13.0 and two stage model ages $t_{Hf(C)} < 1.64$ Ga (Fig. 4). The majority of Devonian and Carboniferous zircons are characterized by deeply negative $\varepsilon_{Hf(t)}$ from –20.0 to –11.6, and two stage model ages $t_{Hf(C)} > 1.73$ Ga. Only one grain in sample V-135 with an age of 381 Ma has a positive $\varepsilon_{Hf(t)} = 5.2$ and two stage model age of $t_{Hf(C)} = 0.90$ Ga (Fig. 4a).

THE RESULTS OF SM–ND ISOTOPE STUDIES

The results of Sm–Nd whole-rock isotope studies of sedimentary rocks are given in Table 3. These data indicate that all studied samples are characterized by deeply negative values of $\varepsilon_{Nd(t)}$ from –11.9 to –6.6 and Paleoproterozoic values of two-stage model ages $t_{Nd(C)} > 1.70$ Ga.

DISCUSSION

With allowance for the obtained new data on zircons from three samples (V-135, V-140, and V-141) and seven previously analyzed samples (V-14, V-18, V-22, V-56, V-57, V-73, V-94 [47]), the U–Pb and Lu–Hf isotope studies involved two samples from the Afanas'ev, Talyma, Zlatoust, and Sagur formations and one sample from the Tokur and undivided Ekimchan + Bokontia formations. The results from dating of detrital zircons shown in Figs. 3a–3h revealed cardinal differences in zircon ages in the probability diagrams for sample pairs taken from the same (Afanas'ev, Talyma, Zlatoust, and Sagur) formations. This fact suggests that these formations contain rocks of different aged. Sharp differences are also observed in Lu–Hf isotope characteristics between samples from the same formations (Fig. 4a–4h). On the other hand, the relative-age probability diagrams and Lu–Hf isotope composition of zircons in samples from the Tokur and Ekimchan+Bokontia formations are practically identical (Figs. 3i, 3j, 4i. 4j). To avoid confusion, below we will operate with sample numbers and their groups, without assignment to definite formations.

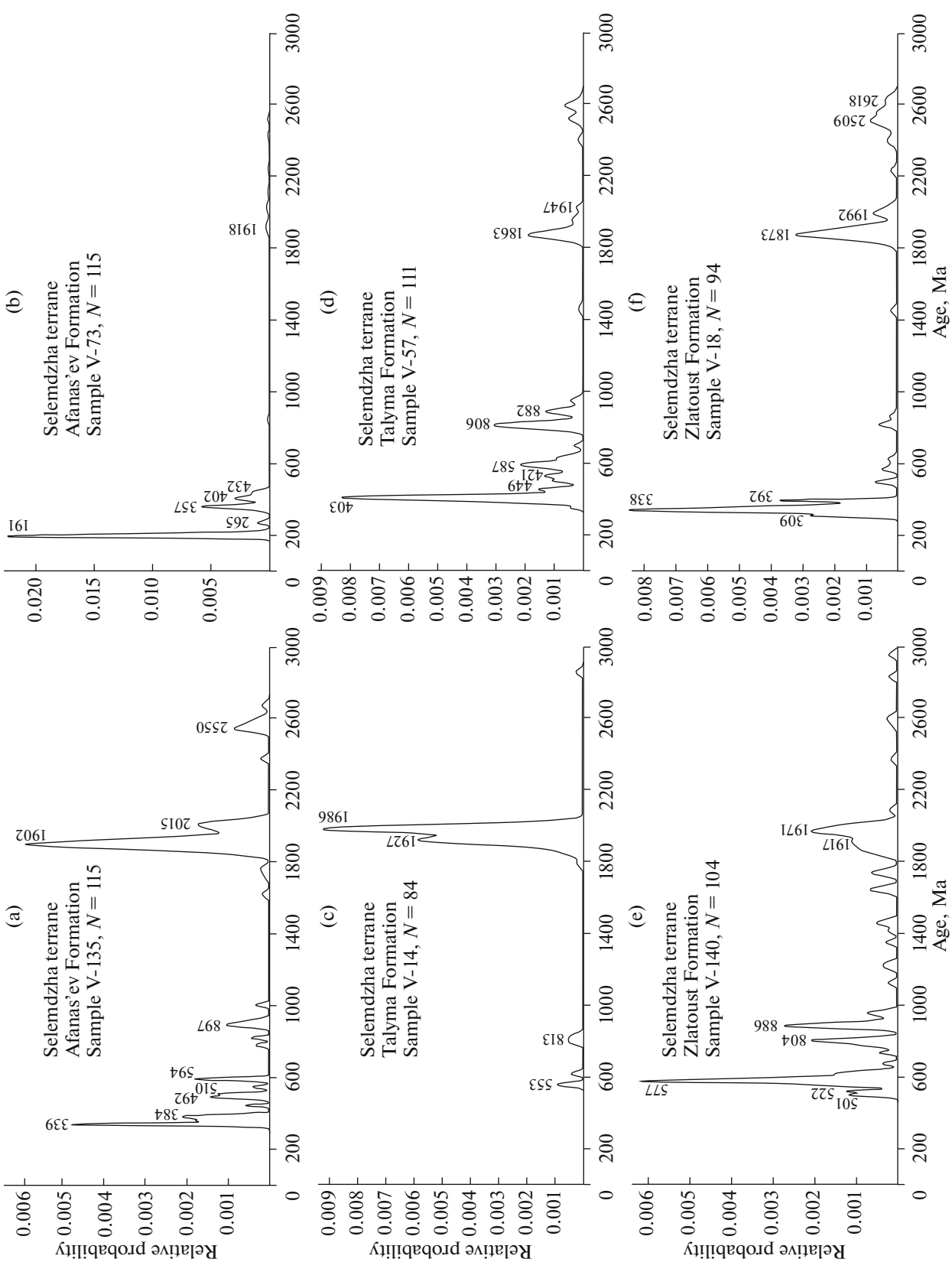

Fig. 3. Relative-age probability diagrams of U–Pb ages for detrital zircons from metasedimentary rocks of the Selemdzha (a–h) and Tokur (i, j) terranes. Sample numbers correspond to numbers in the text. Results for samples V-14, V-18, V-22, V-56, V-57, V-73, V-94 are taken from [47].

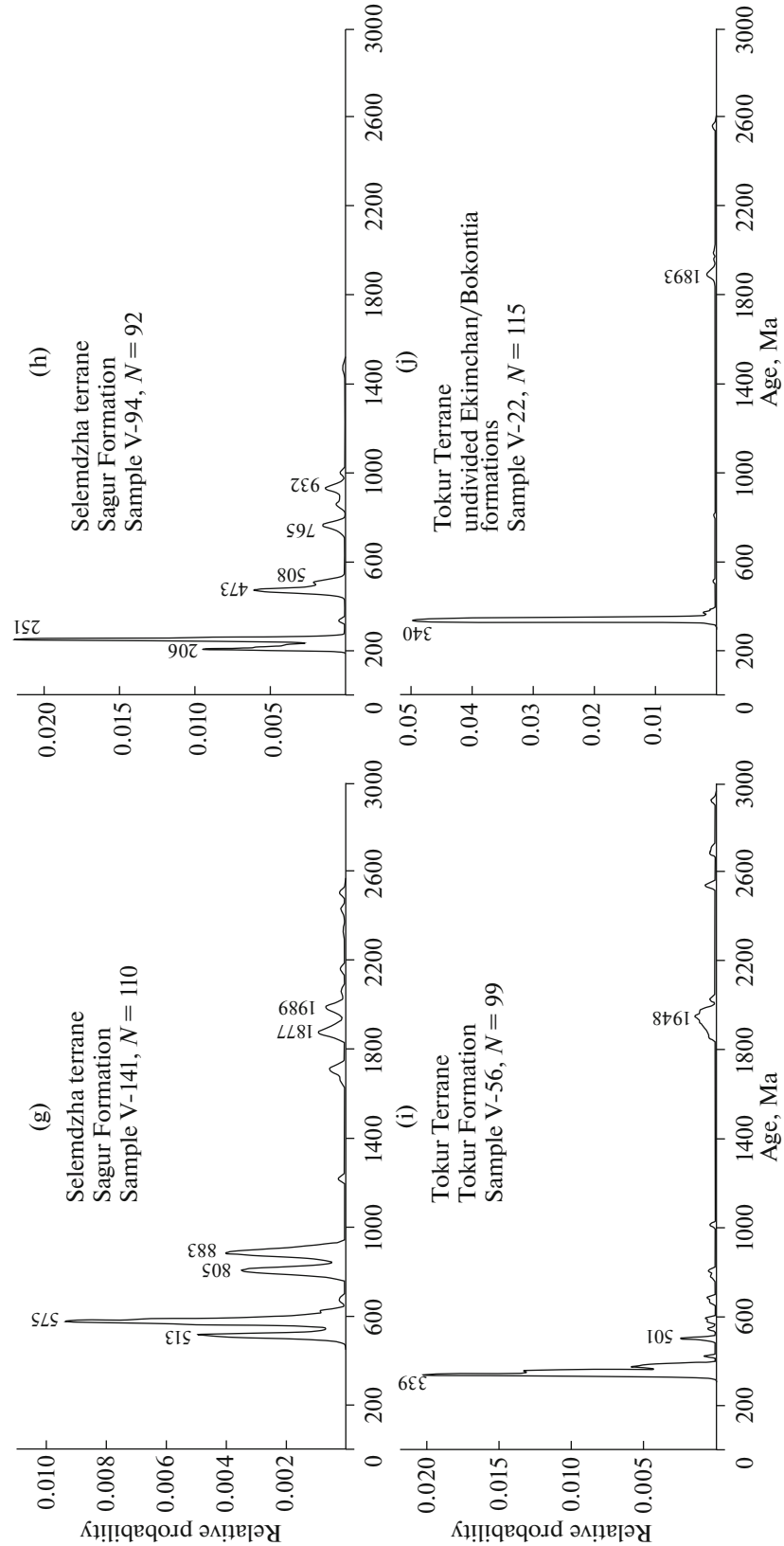
(g)
Selemdzha terrane
Sagur Formation
Sample V-141, N = 110
(h)
Selemdzha terrane
Sagur Formation
Sample V-94, N = 92
(i)
Tokur Terrane
Tokur Formation
Sample V-56, N = 99
(j)
Tokur Terrane
undivided Ekimchan/Bokontia formations
Sample V-22, N = 115
Relative probability
Age, Ma
575
513
805
883
1877
1989
251
206
473
508
765
932
339
501
1948
340
1893

Fig. 3. (Contd.)

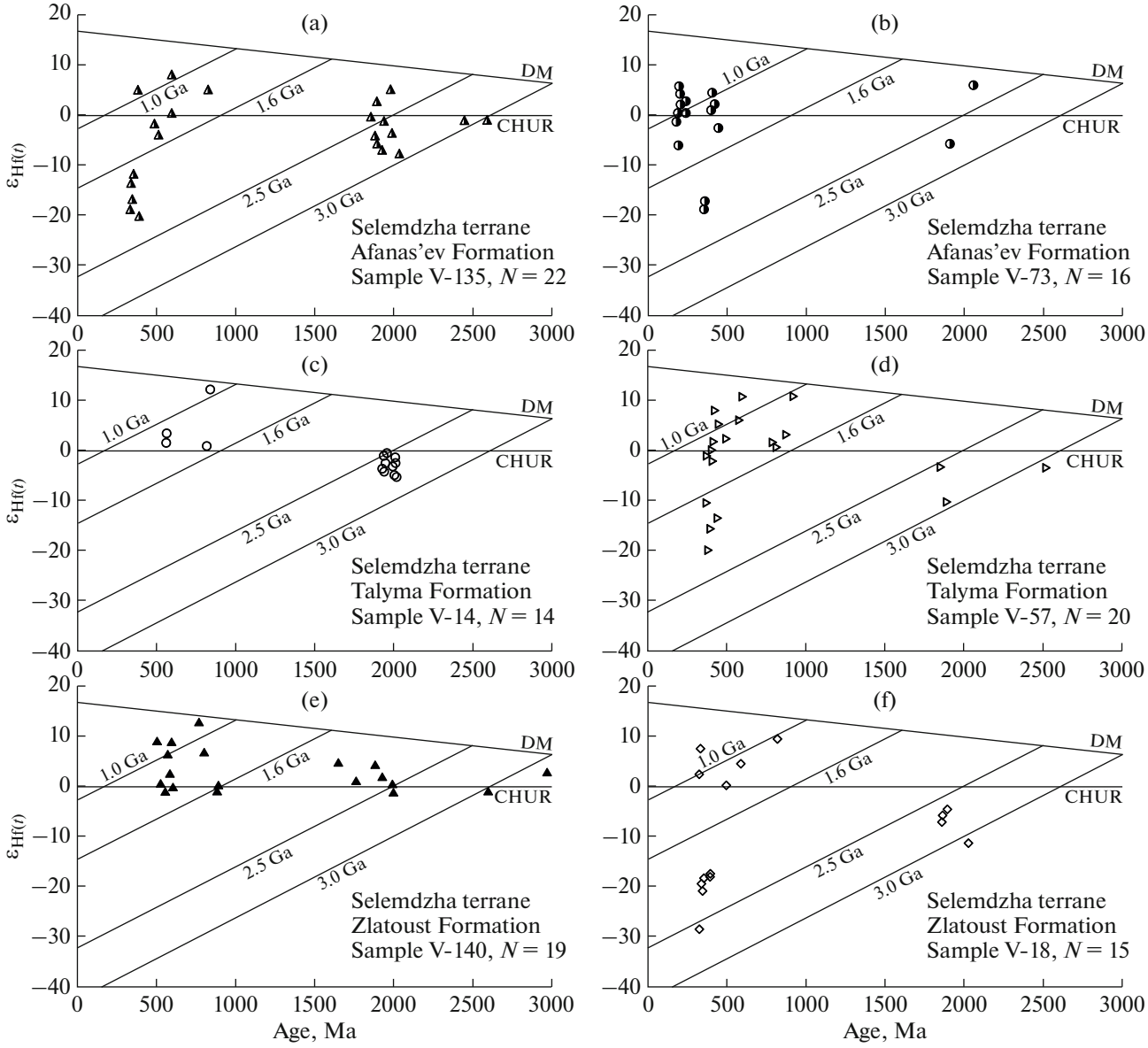

Fig. 4. The $\varepsilon_{Nd(t)}$–age (Ma) diagram for zircons from metasedimentary rocks of the Selemdzha (a–h) and Tokur (i, j) terranes. Sample numbers correspond to numbers in text. (DM) depleted mantle, (CHUR) chondrite uniform reservoir. Results for samples V-14, V-18, V-22, V-56, V-57, V-73, V-94 were taken from [47].

Based on the obtained and available [47] Sm–Nd isotope characteristics (Table 3), U–Pb age (Fig. 3), and Lu–Hf composition of detrital zircons (Fig. 4), the metasedimentary rocks of the Selemdzha and Tokur terranes are roughly divided into two groups.

The largest group (samples V-14, V-18, V-22, V-56, V-57, V-135, V-140, V-141, hereinafter, group I) includes samples with deeply negative values $\varepsilon_{Nd(t)}$ from –18.0 to –6.6 and two-stage model ages $T_{Nd(C)} > 1.68$ Ga. These samples contain numerous Early Precambrian detrital zircons; thus, the absolute majority of zircons, regardless of their crystallization age, have negative or near-zero values of $\varepsilon_{Hf(t)}$ and values of two-stage ages $t_{Nd(C)} > 1.70$ Ga. At the same time, it is necessary to note that some samples contain insignificant amounts of Neoproterozoic, Cambrian, Devonian, and Carboniferous zircons with positive $\varepsilon_{Nd(t)}$ up to +12.3 and two stage model ages $t_{Nd(C)} < 1.60$ Ga.

Weakly negative $\varepsilon_{Nd(t)}$ from –4.2 to –3.9 and two-stage Nd model ages $t_{Nd(C)} < 1.33$ Ga were obtained only for a few samples (samples V-73 and V-94, hereinafter, group II). In these samples, the Early Precambrian zircons are either completely absent or do not form statistically significant populations. The absolute majority of Paleozoic and all Mesozoic zircons have

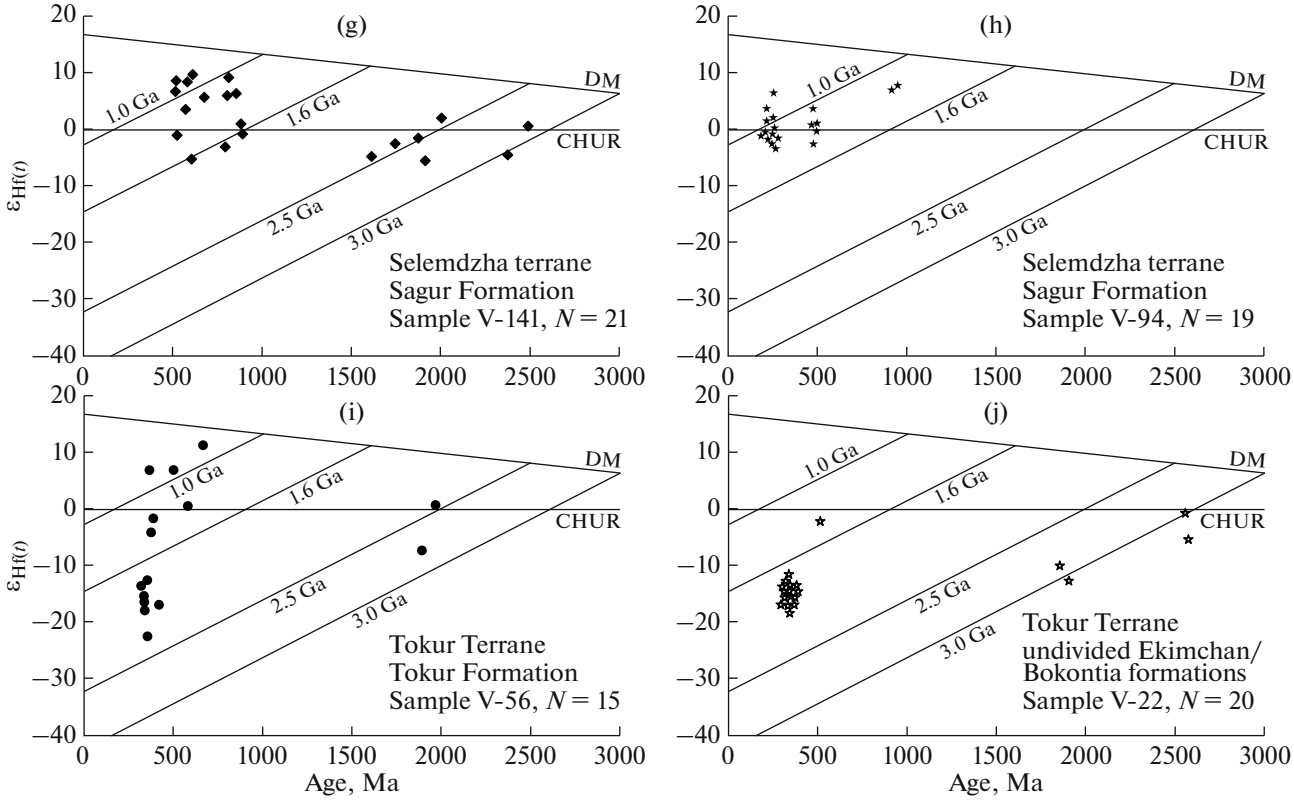

Fig. 4. (Contd.)

$\varepsilon_{Nd(t)} > -2.5$ and two-stage Nd-model ages $t_{Nd(C)} < 1.37$ Ga.

Following this idea with allowance for new data, we attempted (1) to divide sample groups additionally by the age of the youngest zircon population, which determines the lower age limit of deposition, and (2) and to propagate the principles of this grouping to typification of deposits.

To sum up, the following succession of metasedimentary rocks within the Selemdzha and Tokur terranes is proposed.

I-1-type deposits characterized by samples V-14, V-140, V-141, with the lower age limit at 553–498 Ma (Late Ediacaran–Cambrian).

I-2-type deposits characterized by sample V-57, with the lower age limit of deposition at ~373 Ma (Late Devonian).

I-3-type deposits (samples V-22, V-56, V-135) with the lower age limit of deposition of 333–327 Ma (Late Mississippian).

I-4-type deposits (sample V-18) with the lower age limit of deposition at ~304 Ma (Pennsylvanian).

Type-II deposits, which are characterized by samples V-73 and V-94 and have the lower age limit of 202–180 Ma (Late Triassic–Early Jurassic), cannot be subdivided using available information.

It should be noted that such a succession is conceptual and cannot be directly correlated with the stratones of the Selemdzha and Tokur terranes distinguished previously [12, 19, etc.] using the lithological–stratigraphic approach. This can be demonstrated by several examples. In particular, the oldest maximum age of the rocks (553–498 Ma) was established for samples V-14, V-140, and V-141, which according to our classification are ascribed to I-1-type deposits. Thus, none of them was collected from the Afanas'ev Formation, which is considered to compose the base of the general section [12] (Fig. 2). In contrast, samples V-135 and V-73 that we collected from the field of the Afanas'ev Formation (Fig. 2) are biotite–muscovite–quartz–albite schists typical of this formation. However, the youngest zircons from these samples have ages of 333 and 180 Ma, respectively, which determine the maximum age of these samples. Thus, these deposits are not the oldest rocks, as inferred for the Afanas'ev Formation.

At the same time, Sm–Nd, U–Pb, Lu- Hf isotope data provide insight into regional geological problems at a new level. In this regard, our attention should be focused on the following aspects:

(1) I-1-type deposits with the lower deposition limit of 553–498 Ma (Late Ediacaran–Cambrian) could likely be correlated with deposits ascribed to the Olga succession in the Paukan fault zone, which con-

Table 3. The results of Sm-Nd isotope studies of metasedimentary rocks of the Selemdzha and Tokur terranes.

Ordinal no.	Sample no.	Formation	Rock	Age*, Ma	Sm, ppm	Nd, ppm	$^{147}Sm/^{144}Nd$	$^{143}Nd/^{144}Nd$	Err**	$\varepsilon_{Nd(0)}$	$\varepsilon_{Nd(t)}$	$t_{Nd(DM)}$	$t_{Nd(C)}$	Note
1	V-14	Talyma	Metasiltstone	553	5.48	28.33	0.1170	0.512059	2	−11.3	−5.7	1718	1755	This study
2	V-18	Zlatoust	Metasiltstone	304	5.10	27.85	0.1108	0.511928	2	−13.8	−10.5	1806	1953	[47]
3	V-22	Undivided Ekimchan and Bokontia formations	Metasiltstone	329	5.57	30.93	0.1088	0.511875	2	−14.9	−11.2	1849	2030	[47]
4	V-22-3	Undivided Ekimchan and Bokontia formations	Metasiltstone	329	6.62	37.13	0.1077	0.511788	2	−16.6	−12.9	1954	2166	[47]
5	V-56	Tokur	Metasandstone	327	5.24	30.19	0.1050	0.511713	6	−18.0	−14.2	2010	2277	[47]
6	V-57	Talyma	Metasiltstone	373	5.79	29.88	0.1172	0.512106	2	−10.4	−6.6	1647	1685	[47]
7	V-64	Tokur	Metasandstone	327	4.13	21.85	0.1142	0.512028	2	−11.9	−8.5	1716	1802	[47]
8	V-73	Afanas'ev	Two-mica schist	180	5.24	28.99	0.1092	0.512322	3	−6.2	−4.2	1208	1326	[47]
9	V-74	Afanas'ev	Two-mica schist	180	5.86	29.57	0.1199	0.512377	2	−5.1	−3.3	1256	1258	[47]
10	V-75-1	Talyma	Metasiltstone	553	2.72	16.35	0.1006	0.511820	9	−16.0	−9.2	1789	2044	[47]
11	V-77	Zlatoust	Metasiltstone	304	4.60	28.10	0.0989	0.511645	2	−19.4	−15.6	1993	2370	[47]
12	V-94	Sagur	Metasiltstone	202	1.76	7.60	0.1403	0.512362	7	−5.4	−3.9	1636	1326	[47]
13	V-98-1	Undivided Ekimchan and Bokontia formations	Metasiltstone	329	2.48	13.05	0.1148	0.511766	6	−17.0	−13.6	2126	2226	[47]
14	V-99	Undivided Ekimchan and Bokontia formations	Metasiltstone	329	2.11	11.55	0.1105	0.511815	3	−16.1	−12.4	1967	2132	[47]
15	V-101	Tokur	Metasiltstone	327	3.71	20.84	0.1077	0.511759	2	−17.2	−13.4	1995	2213	[47]
16	V-135	Afanas'ev	Two-mica schist	333	3.20	18.01	0.1074	0.511833	4	−15.7	−11.9	1884	2092	This study
17	V-140	Zlatoust	Metasiltstone	501	3.74	21.55	0.1049	0.512053	5	−11.4	−5.5	1536	1702	This study
18	V-141	Sagur	Metasiltstone	498	4.71	24.21	0.1176	0.512077	3	−10.9	−5.9	1700	1730	This study

* Isotope parameters were calculated for an age of the youngest zircon population; ** measurement error of $^{143}Nd/^{144}Nd$ are given at 2σ level.

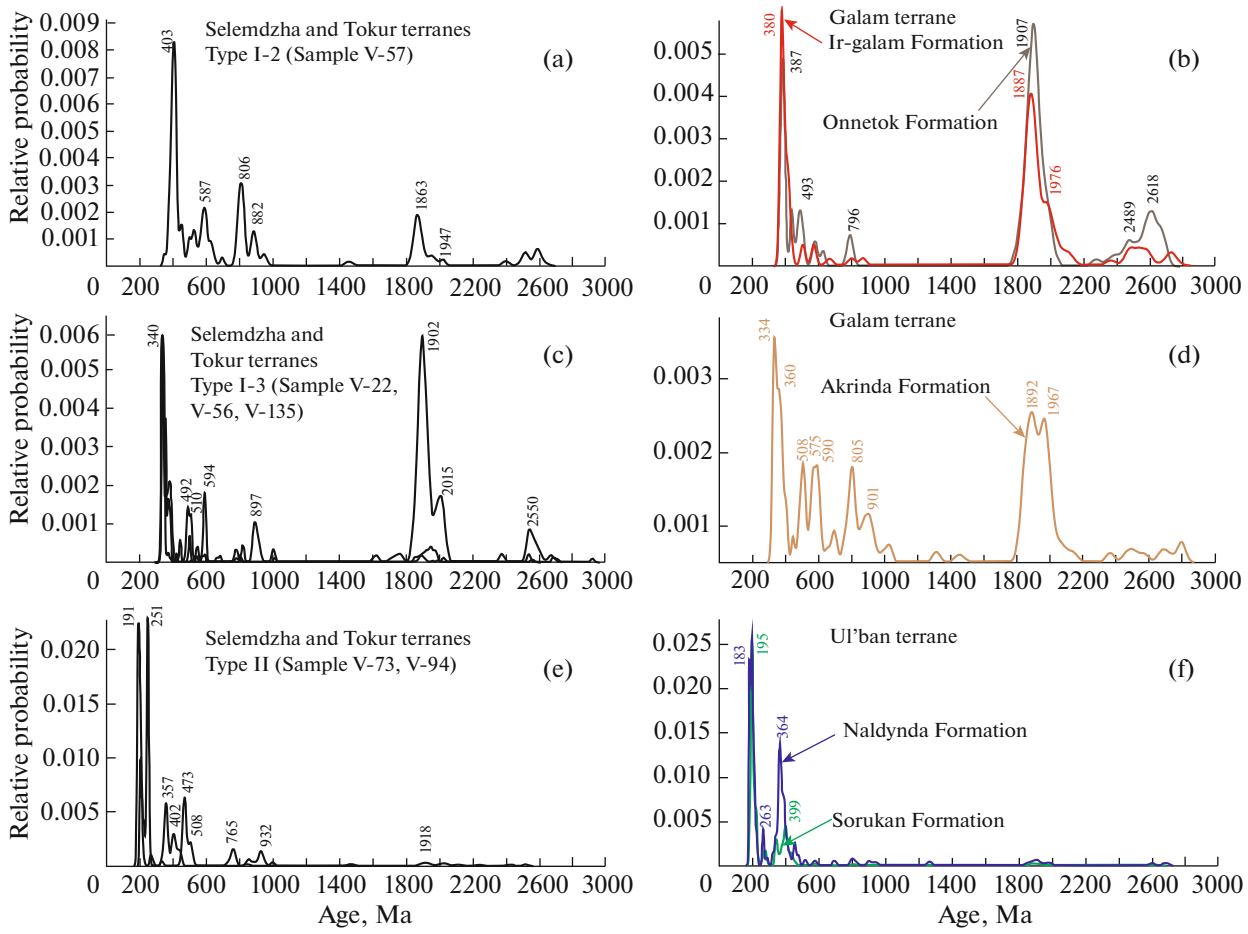

Fig. 5. Relative-age probability diagrams of U–Pb ages for detrital zircons from metasedimentary rocks of types I-2, I-3, and II of the Selemdzha and Tokur terranes compared to possible analogues. Data on the Ir-Galam, Onnetok sequences and Akrinda Formation of the Galam terrane were taken from [11], those on the Sorukan and Naldynda formations from the Ul'ban terrane, were taken from [8].

tain the Early Cambrian skeletal fauna [12]. Thus, it is highly probable that the rocks with the Early Cambrian fauna and Late Ediacaran–Cambrian detrital zircons represent tectonic blocks in the younger rocks.

(2) In the traditionally distinguished stratones of the Selemdzha and Tokur terranes [12, 19, etc.], the fossil fauna and flora were not found, except for find of the Visean–Moscovian spore-pollen assemblage in the siltstones of the Zlatoust Formation [1, 12]. According to our classification, these deposits are ascribed to type I-3 with the lower age limit at 333–327 Ma (Late Mississippian) or type I-4 with the lower age limit at ~304 Ma (Pennsylvanian).

(3) Deposits similar to types I-2 and I-3 in the Selemdzha and Tokur terranes, according to the relative age probability diagrams (Figs. 5a–5d) and Lu–Hf isotope parameters (Figs. 6a–6d) for detrital zircons, were found in the Galam terrane, while deposits similar to type II were found in the Ul'ban terrane (Figs. 5e, 5f; 6e, 6f).

(4) The granitoids of the Ingagli Complex that cut across the deposits of the Tokur terrane are dated within 254–251 Ma [1–3, 12, 41], which is consistent with our data on the lower age limit of 333–327 Ma (Late Mississippian) for the deposition of rocks in this terrane. This is also the case for the Zlatoust Complex. Available age data on the intrusions of this complex are within 257–250 Ma [41]. Thus, the intrusions of the Zlatoust Complex could intrude the deposits of the Selemdzha terrane with the lower age limit ~304 Ma (Pennsylvanian). The only date of 393 ± 7 Ma obtained for a small granite body [41] from fault zone does not place any constraints, but serves as additional evidence for the presence of ancient blocks in the Selemdzha terrane.

To sum up the obtained and available data [9, 11, 47], we proposed a tectono-stratigraphic scheme for the eastern Mongol–Okhotsk belt (Fig. 7) based on Sm–Nd, U–Pb, and Lu–Hf isotope studies. In this scheme, we distinguish tectonic sheets formed by deposits of different types (I-1, I-2, I-3, I-4, and II),

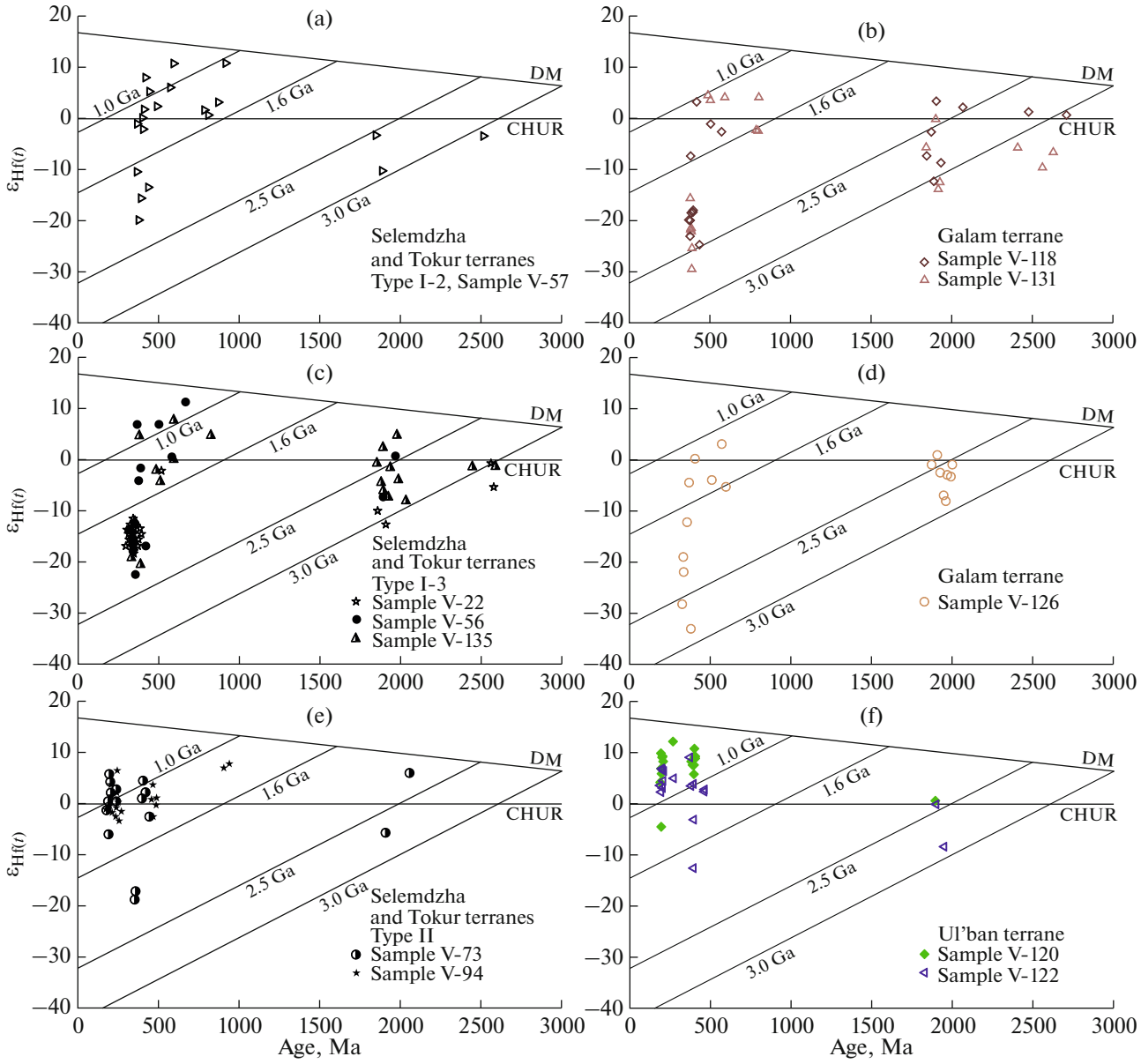

Fig. 6. The $\varepsilon_{Nd(t)}$–age (Ma) diagram for zircons from metasedimentary rocks of types I-2, I-3, and II of the Selemdzha and Tokur terranes compared to possible analogues. Data on the Ir-Galam, Onnetok sequences and Akrinda Formation of the Galam terrane were taken from [11], those on the Sorukan and Naldynda formations of the Ul'ban terrane, from [8].

i.e., having different Sm–Nd and Lu–Hf isotope parameters, as well as different lower age limits. These sheets have a composite inner structure and can be considered as tectono-stratigraphic units.

Assuming that the rocks with the Early Paleozoic lower age limit (type I-1sediments) are tectonic blocks in the younger rocks (in I-4-type sediments), the age of the tectonostratigraphic units from the north southward decreases: I-2 → I-3 → I-4 (Fig. 7). With allowance for the fault dip to the north, a similar trend is also observed from top downward (from upper to lower sheets). Such structure is typical of accretionary wedge terranes with the rear part in the north and frontal part in the south. This trend indicates that the tectonostratigraphic units formed by type-I deposits (including the I-1, I-2, I-3, and I-4 types) and previously ascribed to the Selemdzha and Tokur terranes [21] likely belong to the Galam accretionary wedge terrane of the Mongol–Okhotsk belt (after [17]) or to the Galam accretionary wedge terrane of the Okhotsk–Koryak orogenic belt (after [5, 33]).

In the south, in its frontal part, the tectonostratigraphic units formed by type-I deposit via fault system are juxtaposed with tectonostratigraphic units of type II (Fig. 7), which are ascribed to other accretionary system formed in front of the Amur superterrane

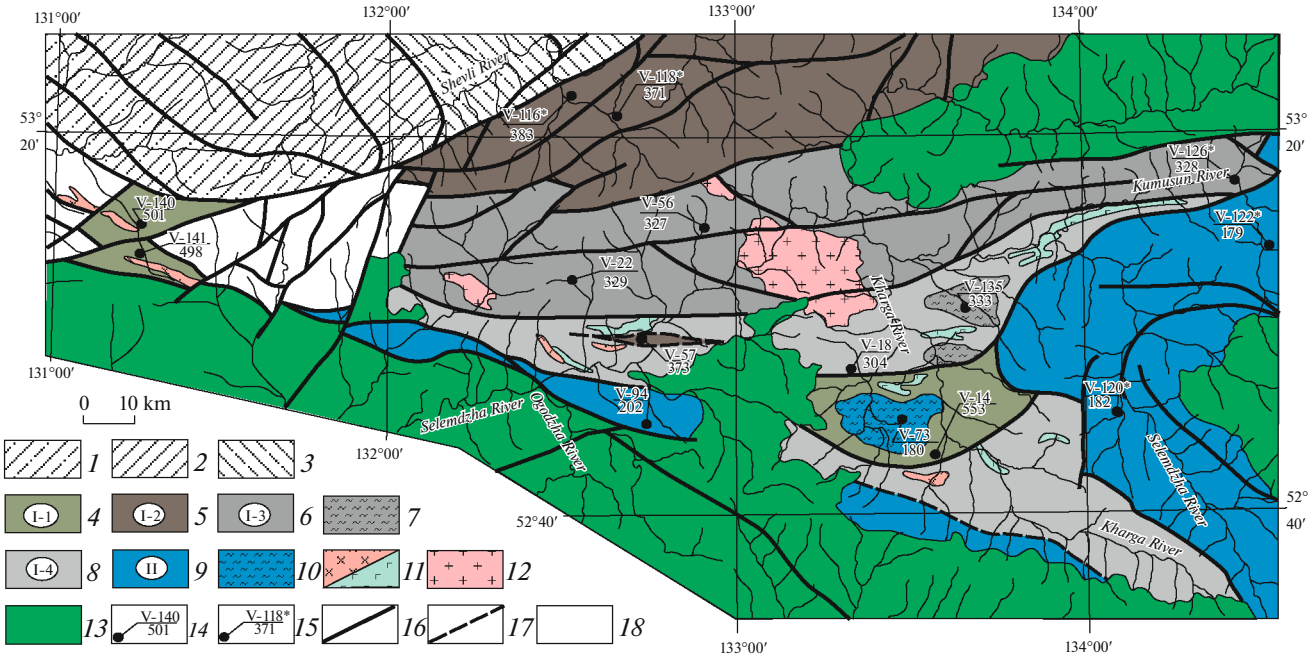

Fig. 7. The tectonostratigraphic scheme of the eastern Mongol–Okhotsk orogenic belt (excluding Early and Late Cretaceous intrusive complexes). (*1–3*) structures bordering the Tokur, Selemdzha, and Galam terranes: (*1*) Paleozoic (?) complexes of the Dzhagdy terrane; (*2*) Early Mesozoic complexes of the Un'ya-Bon terrane; (*3*) Paleozoic and Early Mesozoic complexes of the Lan terrane; (*4–10*) tectonostratigraphic units: (*4*) type I-1 deposits with lower age limit at 553–498 Ma (Late Ediacaran–Cambrian); (*5*) type I-2 deposits with the lower age limit at ~373 Ma (Late Devonian); (*6*) type I-3 deposits with the lower age limit at 333–327 Ma (Late Mississippian); (*7*) type I-3 deposits in erosion windows; (*8*) type I-4 deposits with the lower age limit at ~304 Ma (Pennsylvanian); (*9*) type II deposits with the lower age limit at 202–180 Ma (Late Triassic–Early Jurassic); (*10*) type II deposits in erosion windows; (*11*) Late Paleozoic gabbroplagiogranite of the Zlatoust Complex; (*12*) Late Paleozoic Ingagli granitoid complex; (*13*) Early Cretaceous volcanic and subvolcanic complexes; (*14*) sampling localities for U–Pb geochronological and Lu-Hf isotope studies. Their numbers (in nominator) and age of the youngest zircon population (in denominator); (*15*) the same, taken from literature data [8, 11]; (*16*) main faults; (*17*) inferred faults; (*18*) uncertainty field.

margin. At present, it is too early to discuss the kinematics of relations of two different accretionary systems; however, it is obvious that their formation was not instantaneous.

CONCLUSIONS

Our study allowed us to draw the following conclusions:

(1) The results from U–Pb, Lu–Hf, and Sm–Nd isotope studies of metasedimentary rocks in the Selemdzha and Tokur terranes of the Mongol–Okhotsk belt highlighted a need for the revision of stratigraphic principles of mapping within the belt. At the same time, we do not diminish the qualifications or the experience of the geologists that mapped this area previously.

(2) The Selemdzha and Tokur terranes contain two types of deposits, which cardinally differ in Sm–Nd whole-rock isotope parameters and Lu–Hf isotope composition of detrital zircons. Type-I deposits are characterized by samples with very negative $\varepsilon_{Nd(t)}$ from –18.0 to –6.6 and two-stage Nd model ages $T_{Nd(C)} >$ 1.68 Ga. These deposits contain numerous Early Precambrian detrital zircons; thus, the majority of zircons, regardless of their crystallization age, have negative or near-zero values of $\varepsilon_{Nd(t)}$ and two-stage model ages of $T_{Nd(C)} > 1.70$ Ga. The type-II deposits are characterized by samples with weakly negative $\varepsilon_{Nd(t)}$ from –4.2 to –3.9 and two-sage Nd-model ages $T_{Nd(C)} <$ 1.33 Ga. In these deposits, the Early Precambrian zircons are either absent or do not form statistically significant populations. The majority of Paleozoic and all Mesozoic zircons have $\varepsilon_{Nd(t)} > -2.5$ and two-stage model ages of $T_{Nd(C)} < 1.37$ Ga. The deposits of different types are involved in the formation of two opposite accretionary systems: in front of the margin of the Siberian Craton (type I deposits) and Amur superterrane (type II deposits).

(3) The type-I deposits are divided into discrete groups, which differ in the lower age limit: I-1 (553–498 Ma, Late Ediacaran–Cambrian); I-2 (~373 Ma, Late Devonian); I-3 (333–327 Ma, Late Mississippian); and I-4 (~304 Ma, Pennsylvanian). Assuming that the rocks with the Early Paleozoic lower age limit are tectonic blocks in the younger rocks, from the north southward the age of the deposits (tectonostratigraphic units) decreases in the following succes-

sion: I-2 → I-3 → I-4. A similar age decrease is also observed from the upper to lower sheets. Such a structure is typical of accretionary wedge terranes with their rear part in the north and frontal part in the south.

(4) Tectonostratigraphic units formed by type-I deposits and previously ascribed to the Selemdzha and Tokur terranes likely belong to the Galam accretionary-wedge terrane.

(5) The kinematics of the relationships of two opposite accretionary systems made up of different tectonostratigraphic units (types I and II deposits) have not been deciphered as yet. However, it is obvious that these relationships were not instantaneous.

ACKNOWLEDGMENTS

We are grateful to E.N. Voropaeva, O.G. Medvedeva (Institute of Geology and Nature Management of FEB RAS, Blagoveshchensk) for the preparation of monomineral zircon fractions.V.P. Kovach and N. Y. Zagornaya (Institute of Precambrian Geology and Geochronology, RAS) are thanked for the performance of Sm–Nd isotope studies, and the staff of the LaserChron Center of the Arizona University (USA), for the performance of U–Pb and Lu–Hf isotope studies.

We also thank Academician A.I. Khanchuk, as well as G.L. Kirilova, and I.A. Aleksandrova for comments and recommendations, which significantly improved the manuscript.

FUNDING

These studies were supported by the Russian Science Foundation (project no. 18-17-00002).

CONFLICT OF INTEREST

The authors declare that they have no conflicts of interest.

SUPPLEMENTARY INFORMATION

The online version contains supplementary material available at https://doi.org/10.1134/S181971402204008X

Supplements_1, 2 are available at http://itig.as.khb.ru/POG/2022/n4/pdf/Zaika.pdf

REFERENCES

1. S. G. Agafonenko, *State Geological Map of the Russian Federation. 1 : 200000. 2nd Edition. Tugur Series. Sheet N-53-XXVI (Zlatoustovsk)*, Ed. by A.V. Makhinin (VSEGEI, St. Petersburg, 2015) [in Russian].
2. S. G. Agafonenko, A. N. Serezhnikov, and A. L. Yashnov, *State Geological Map of the Russian Federation. 1 : 200000. 2nd Edition. Tugur Series. Sheet N-53-XXV (Ekimchan)*, Ed. by A.V. Makhinin (VSEGEI, St. Petersburg, 2019) [in Russian].
3. S. G. Agafonenko, A. N. Serezhnikov, and A. L. Yashnov, *State Geological Map of the Russian Federation. 1 : 200000. 2nd Edition. Tugur Series. Sheet N-52-XXX (Stoiba),* Ed. by A.V. Makhinin (VSEGEI, St. Petersburg, 2019) [in Russian].
4. A. F. Vas'kin, *Geological Map of the BAM Region. 1 : 500000. Sheet N-53-V*,, Ed. by M. T. Turbin (VSEGEI, Leningrad, 1984) [in Russian].
5. *Geodynamics, Magmatism. and Metallogeny of East Russia*, Ed. by A. I. Khanchuk (Dal'nauka, Vladivostok, 2006) [in Russian].
6. G. S. Gusev and V. E. Khain, "Relations of the Baikal–Vitim, Aldan–Stanovoy, and Mongol–Okhotsk terranes (southern Middle Siberia)," Geotektonika, No. **5**, 68–82 (1995).
7. A. K. Egorov, *Geological Map of the USSR. 1 : 200000. Tugur Series. Sheet N-53-XXV*, Ed. by E.L. Shkol'nik (VSEGEI, Leningrad, 1968) [in Russian].
8. V. A. Zaika and A. A. Sorokin, "Tectonic nature of the Ul'ban terrane (Mongol–Okhotsk Fold Belt): Results of U–Pb and Lu–Hf isotope studies of detrital zircons," Dokl. Earth Sci. **492** (1), 297–301 (2020).
9. V. A. Zaika and A. A. Sorokin, "Ages and sources of sedimentary rocks of the Lan Terrane in the Mongol–Okhotsk Fold Belt: Results of zircon U–Pb and Lu–Hf isotope studies," Russ. J. Pac. Geol. **39** (3), 193–205 (2020).
10. V. A. Zaika, A. A. Sorokin, V. P. Kovach, and A. B. Kotov, "Geochemistry of metasedimentary rocks, sources of clastic material, and tectonic nature of Mesozoic basins on the northern framing of the eastern Mongol–Okhotsk orogenic belt," Russ. Geol. Geophys. **61** (3), 286–301 (2020). https://doi.org/10.15372/RGG2019095
11. V. A. Zaika and A. A. Sorokin, "Age and sources of metasedimentary rocks of the Galam terrane in the Mongol–Okhotsk Fold Belt: Results of U–Pb age and Lu–Hf isotope data from detrital zircons," Geotectonics **55** (6), 779–794 (2021).
12. V. Yu. Zabrodin, V. A. Gur'yanov, S. G. Kislyakov, et al., *State Geological Map of the Russian Federation. 1 : 1000000. Far East Series. Sheet N-53. Third Generation* (VSEGEI, St. Petersburg, 2007) [in Russian].
13. L. P. Zonenshain, M. I. Kuz'min, and L. M. Natapov, *Tectonics of Lithospheric Plates of the USSR Territory* (Nedra, Moscow, 1990), **Vol. 1** [in Russian].
14. V. F. Zubkov, *Geological Map of the USSR. 1 : 200000. Tugur Series. Sheet N-53-XXVI*, Ed. by S.A. Muzylev (VSEGEI, Leningrad, 1981) [in Russian].
15. V. F. Zubkov and M. T. Turbin, *Geological Map of the BAM Region. 1 : 500000. N-52-G*, Ed. by M.G. Zolotov (VSEGEI, Leningrad, 1984) [in Russian].
16. L. I. Krasnyi, and Pen Yun'byao, *Geological Map of the Amur Region and Adajacent Territories. 1 : 2500000*, Ed. by L. I. Krasnyi (VSEGEI, St. Petersburg, 1999) [in Russian].
17. L. M. Parfenov, L. I. Popeko, and O. Tomurtogoo, "Problems of tectonics of the Mongol–Okhotsk orogenic belt," Tikhookean. Geol. **18** (5), 24–43 (1999).
18. L. M. Parfenov, N. A. Berzin, A. I. Khanchuk, G. Badarch, V. G. Belichenko, A. N. Bulgatov, S. I. Dril', G. L. Kirillova, M. I. Kuz'min, U. Nokleberg, A. V. Prokop'ev, V. F. Timofeev, O. Tomurtogoo, and H. Yan, "Model of formation of orogenic belts of cen-

tral and northeastern Asia," Tikhookean. Geol. **22** (6), 7–41 (2003).

19. A. N. Serezhnikov and Yu. R. Volkova, *State Geological Map of the Russian Federation. 1 : 1000000. Third Generation. Sheet N-52 (Zeya). Far East Series*,, Ed. by A.S. Vol'skii (VSEGEI. St. Petersburg, 2007) [in Russian].
20. Yu. N. Smirnova, A. A. Sorokin, L. I. Popeko, A. B. Kotov, and V. P. Kovach, "Geochemistry and provenances of the Jurassic terrigenous rocks of the Upper Amur and Zeya–Dep troughs, eastern Central Asian Fold Belt," Geochem. Int. **55** (2), 163–183 (2017).
21. A. A. Sorokin, N. M. Kudryashov, A. P. Sorokin, A. G. Rublev, O. A. Levchenkov, A. B. Kotov, E. B. Sal'nikova, and V. P. Kovach, "Geochronology, geochemistry, and geodynamic setting of Paleozoic granitoids in the eastern segment of Mongol–Okhotsk Belt," Dokl. Earth Sci. **393** (8), 1136–1140 (2003).
22. Yu. I. Shcherbina, *Geological Map of the USSR. 1 : 200000. Tugur Series. Sheet N-52-XXKh*, Ed. by E.L. Shkol'nik (VSEGEI, Leningrad, 1974) [in Russian].
23. L. P. Black, S. L. Kamo, C. M. Allen, D. W. Davis, J. N. Aleinikoff, J. W. Valley, R. Mundil, I. H. Campbell, R. J. Korsch, I. S. Williams, and C. Foudoulis, "Improved $^{206}Pb/^{238}U$ microprobe geochronology by the monitoring of trace-element-related matrix effect: SHRIMP, ID-TIMS, ELA-ICP-MS and oxygen isotope documentation for a series of zircon standards," Chem. Geol. **205**, 15–140 (2004). https://doi.org/10.1016/j.chemgeo.2004.01.003
24. J. Blichert-Toft and F. Albarede, "The Lu–Hf geochemistry of chondrites and the evolution of the mantle–crust system," Earth Planet. Sci. Lett. **148**, 243–258 (1997).
25. D. Bussien, N. Gombojav, W. Winkler, and A. Quadt, "The Mongol–Okhotsk belt in Mongolia - an appraisal of the geodynamic development by the study of sandstone provenance and detrital zircons," Tectonophysics **510**, 132–150 (2011).
26. E. I. Demonterova, A. V. Ivanov, E. A. Mikheeva, A. V. Arzhannikova, A. O. Frolov, S. G. Arzannikov, N. V. Bryanskiy, and L. A. Pavlova, "Early to Middle Jurassic history of the southern Siberian continent (Transbaikalia) recorded in sediments of the Siberian Craton: Sm-Nd and U–Pb provenance study," Bull. Soc. Geol. France **188** (1–2), 1–29 (2017). https://doi.org/10.1051/bsgf/2017009
27. G. E. Gehrels, V. Valencia, and J. Ruiz, "Enhanced precision, accuracy, efficiency, and spatial resolution of U–Pb ages by laser ablation–multicollector-inductively coupled plasma-mass spectrometry," Geochem., Geophys., Geosystems **9** (3), 1–13 (2008). https://doi.org/10.1029/2007GC001805
28. S. J. Goldstein and S. B. Jacobsen, "Nd and Sr isotopic systematic of rivers water suspended material: implications for crustal evolution," *Earth Planet Sci. Lett.* **87**, 249–265 (1988).
29. H. Hara, T. Kurihara, K. Tsukada, Y. Kon, T. Uchino, T. Suzuki, M. Takeuchi, Y. Nakane, M. Nuramkhaan, and Minjin Chuluun, "Provenance and origins of a Late Paleozoic accretionary complex within the Khangai–Khentei belt in the Central Asian Orogenic Belt, Central Mongolia," J. Asian Earth Sci. **75**, 141–157 (2013). https://doi.org/10.1016/j.jseaes.2013.07.019
30. S. B. Jakobsen and G. J. Wasserburg, "Sm-Nd evolution of chondrites and achondrites," Earth Planet Sci. Lett **67**, 137–150 (1984).
31. T. K. Kelty, A. Yin, B. Dash, E. George, F. Gehrels, and Angela E. Ribeiro, "Detrital-zircon geochronology of Paleozoic sedimentary rocks in the Hangay–Hentey basin, north-central Mongolia: Implications for the tectonic evolution of the Mongol–Okhotsk ocean in Central Asia," Tectonophysics **451**, 290–311 (2008).
32. L. S. Keto and S. B. Jacobsen, "Nd and Sr Isotopic Variations of Early Paleozoic Oceans," Earth Planet. Sci. Lett. **84**, 27–41 (1987).
33. A. I. Khanchuk, A. N. Didenko, L. I. Popeko, A. A. Sorokin, and B. F. Shevchenko, "Structure and evolution of the Mongol–Okhotsk Orogenic Belt," *The Central Asian Orogenic Belt. Geology, Evolution, Tectonics, and Models*, Ed. by A. Kroner, (Borntraeger Sci. Publ., Stuttgart, 2015, pp. 211–234).
34. K. R. Ludwig, "Isoplot 3.6," Berkeley Geochronol. Center Spec. Publ., No. 4, (2008).
35. J. M. Mattinson, "Analysis of the relative decay constants of ^{235}U and ^{238}U by multi-step CA-TIMS measurements of closed system natural zircon samples," Chem. Geol. **275**, 186–198 (2010). https://doi.org/10.1016/j.chemgeo.2010.05.007
36. B. A. Natal'in, "History and modes of Mesozoic accretion in southeastern Russia," The Island Arc **2**, 15–34 (1993).
37. W. J. Nokleberg, T. K. Bundtzen, R. A. Eremin, V. V. Ratkin, K. M. Dawson, V. I. Shpikerman, N. A. Goryachev, S. G. Byalobzhesky, Y. F. Frolov, A. I. Khanchuk, R. D. Koch, J. W. H. Monger, A. I. Pozdeev, I. S. Rozenblum, S. M. Rodionov, L. M. Parfenov, C. R. Scotese, and A. A. Sidorov, "Metallogenesis and tectonics of the Russian Far East, Alaska, and the Canadian Cordillera," Prof. Pap.-US Geol. Surv., No. 1697, (2005).
38. J. B. Paces and J. D. Miller, "Precise U–Pb ages of Duluth Complex and related mafic intrusions, northeastern Minnesota: geochronological insights to physical, petrogenic, paleomagnetic, and tectonomagmatic processes associated with the 1.1. Ga Midcontinent rift system," J. Geophys. **98** (8), 13997–14013 (1993).
39. D. Ruppen, A. Knaf, D. Bussien, W. Winkler, A. Chimedtseren, and Albrecht Von Quadt, "Restoring the Silurian to Carboniferous northern active continental margin of the Mongol-Okhotsk ocean in Mongolia: Hangay–Hentey accretionary wedge and seamount collision," Gondwana Res **25**, 1517–1534 (2014). https://doi.org/10.1016/j.gr.2013.05.022
40. A. A. Sorokin, V. A. Zaika, V. P. Kovach, A. B. Kotov, W. Xu, "Timing of closure of the eastern Mongol–Okhotsk Ocean: Constraints from U-Pb and Hf isotopic data of detrital zircons from metasediments along the Dzhagdy transect," Gondwana Res. **81**, 58–78 (2020). https://doi.org/10.1016/j.gr.2019.11.009
41. A. A. Sorokin, V. A. Zaika, and N. M. Kudryashov, "Timing of formation and tectonic setting of Paleozoic Granitoids in the eastern Mongol–Okhotsk Belt: Constraints from geochemical, U–Pb, and Hf isotope da-

ta," Lithos **388–389**, 106086 (2021). https://doi.org/10.1016/j.lithos.2021.106086

42. J. S. Stacey and I. D. Kramers, "Approximation of terrestrial lead isotope evolution by a two-stage model," Earth Planet. Sci. Lett. **26** (2), 207–221 (1975).
43. T. Tanaka, S. Togashi, H. Kamioka, H. Amakawa, H. Kagami, T. Hamamoto, M. Yuhara, Y. Orihashi, S. Yoneda, H. Shimizu, T. Kunimaru, K. Takahashi, T. Yanagi, T. Nakano, H. Fujimaki, R. Shinjo, Y. Asahara, M. Tanimizu, and C. Dragusanu, "Jndi-1: a neodymium isotopic reference in consistency with Lajolla Neodymium," Chem. Geol. **168**, 279–281 (2000).
44. Taylor, S.R. and McLennan, S.M., *The Continental Crust: Its Composition and Evolution* (Blackwell, London, 1985).
45. J. D. Vervoort and P. J. Patchett, "Behavior of hafnium and neodymium isotopes in the crust: Constraints from Precambrian crustally derived granites," Geochim. Cosmochim. Acta **60**, 3717–3723 (1996).
46. Z. Yi and J. G. Meert, "A closure of the Mongol–Okhotsk Ocean by the Middle Jurassic: reconciliation of paleomagnetic and geological evidence," Geophys. Rev. Lett. **47**, e2020GL088235 (2020). https://doi.org/10.1029/2020GL088235
47. V. A. Zaika and A. A. Sorokin, "Two types of accretionary complexes in the eastern Mongol–Okhotsk belt: Constraints from U–Pb and Hf isotopic data of detrital zircons from metasedimentary rocks of the Selemdzha and Tokur terranes," J. Asian Earth Sci. **201**, 104508 (2020). https://doi.org/10.1016/j.jseaes.2020.104508

Recommended for publishing by A.I. Khanchuk

Translated by M. Bogina